JOURNAL OF CATALYSIS 148, 438–452 (1994)

FTIR Spectroscopic Study of Thiophene, SO_2, and CO Adsorption on Cu/Al_2O_3 Catalysts

Martin B. Padley,* Colin H. Rochester,* Graham J. Hutchings,† and Frank King‡

*Department of Chemistry, The University, Dundee DD1 4HN, United Kingdom; †Leverhulme Centre for Innovative Catalysis, Chemistry Department, Liverpool University, P.O. Box 147, Liverpool L69 3BX, United Kingdom; and ‡ICI Katalco R & T Group, P.O. Box 1, Billingham, Cleveland TS23 1LB, United Kingdom

Received June 16, 1993; revised February 11, 1994

Infrared spectra are reported of copper/alumina catalysts in various states of oxidation or reduction and exposed to carbon monoxide, thiophene, sulphur dioxide, co-adsorbed carbon monoxide and thiophene, and co-adsorbed carbon monoxide and sulphur dioxide. Available adsorption sites could be broadly divided into four groups: Cu^{2+}, Cu^+ in a matrix of Cu^{2+}, Cu^+ in a matrix of Cu^+, and Cu^0. Both site-blocking and electronic effects of thiophene on CO adsorption have been identified and are discussed in terms of the nature of the surface–adsorbate interactions, the oxidation state of the adsorption sites, and the specific effects of thiophene on the adsorption sites for CO. Sulphur dioxide blocked CO adsorption on Cu^{2+} sites. Adsorption of CO on Cu^+ sites was not inhibited by adsorption of sulphur dioxide, the latter having an electronic effect on CO molecules at adjacent sites. Adsorption of sulphur dioxide on a reduced Cu^0 surface caused surface oxidation giving Cu^+ sites which were available for the subsequent adsorption of CO. The pre-adsorption of CO impeded but did not prevent the oxidative effects of sulphur dioxide chemisorption.

INTRODUCTION

Improved selectivity towards the formation of crotyl alcohol from the hydrogenation of crotonaldehyde over Cu/Al_2O_3 has been induced by predosing the catalyst with small amounts of thiophene (1, 2) or sulphur dioxide (3). Explanations of the influence of sulphur on the adsorptive and catalytic properties of metal surfaces have invoked geometric effects (4–7), electronic effects (8–12), and reconstructions or surface morphology changes (13–15). Sulphur has been shown to occupy high coordination sites at low coverages on Cu(100), Cu(111), and Cu(110) surfaces (16–18). A c(2 × 2) LEED pattern was observed, although further additions of sulphur gave more complex surface structures. The adsorption of thiophene on copper has been reported to be nondissociative up to 300 K (19, 20). Multilayer adsorption at 95 K gave way to a monolayer above 150 K with the molecules parallel to the surface at low coverages but orientated in both parallel and inclined structures at high coverages. Sulphur dioxide is physisorbed at 100–193 K on polycrystalline (21) and single-crystal (22, 23) copper surfaces. There are two reports that sulphur dioxide does not adsorb on copper at 298 K (21, 22). However, EELS of Cu(100) exposed to sulphur dioxide at 300 K contained evidence for adsorbed sulphite species (23). It was suggested that sulphur dioxide dissociated to SO and O on the Cu(100) surface and that further reaction with sulphur dioxide generated adsorbed sulphite and sulphur species. The sulphite decomposed at 370 K to give adsorbed S and O atoms (23).

IR spectroscopy using CO as a probe molecule has given information about the interactions between sulphur compounds and the surfaces of platinum (24, 25) and nickel (26). The present paper reports an IR study of thiophene and sulphur dioxide adsorption and the effects of thiophene and sulphur dioxide on CO adsorption for alumina supported copper catalysts in which surface copper was present as Cu^0, Cu^+, or Cu^{2+} before exposure to CO or thiophene. The reduced catalyst was identical to that used in the studies of crotonaldehyde hydrogenation (1–3).

EXPERIMENTAL

A dispersion of Condea SCF γ-Al_2O_3 (Puralox SCFa-140, surface area 136 $m^2 g^{-1}$) in aqueous copper(II) nitrate was evaporated to dryness at ca. 353 K and dried in air for 16 h at 383 K. The resulting catalyst precursor was compressed at 20 MN m^{-2} into self-supporting discs (100 mg, 25 mm diameter) which were mounted in an infrared cell fitted with fluorite windows and glassblown to a conventional glass vacuum apparatus fitted with grease-free taps.

A disc *in situ* in the infrared cell was raised into the furnace section of the cell at 403 K. A flow (100 $cm^3 min^{-1}$, 0.1 MN m^{-2}) of dry air was passed through the cell as the temperature was raised to 583 K. After 16 h at 583 K the air flow was discontinued and evacuation was started

0021-9517/94 $6.00

with the disc still at 583 K. One of three alternative treatments then preceded the admission of adsorbate gases. First, the disc was cooled to ambient temperature (ca. 295 K) after evacuation (583 K, 1 h) giving catalyst designated "calcined catalyst." Second, the disc was subjected to a sequence of treatments involving evacuation (583 K, 1.5 h then cooling to 323 K over 3 h, cooling to 295 K for spectroscopic examination, heating at 368 K followed by heating to 403 K over 45 min), reduction in a flow of hydrogen (100 cm^3 min^{-1}, 0.1 MN m^{-2}) with the temperature raised to 483 K over 2 h and held at 483 K for 16 h, and finally evacuation (483 K for 1 h) followed by cooling to 295 K giving catalyst designated "reduced catalyst." Third, a reduced copper catalyst disc was exposed to nitrous oxide (4 kN m^{-2}, 353 K, 15 min) before evacuation (353 K, 15 min) and cooling to 295 K gave catalyst designated "Cu/Al_2O_3 (ex N_2O)" with a surface layer of Cu^+ ions on the copper component (27). The copper content of the catalyst precursor was adjusted to give 5 wt.% Cu in reduced Cu/Al_2O_3 catalyst.

A TPR profile for calcined catalyst in hydrogen showed that complete reduction to Cu/Al_2O_3 was effected at 483 K. The Cu surface area (N_2O adsorption at 353 K, reactive frontal chromatography) was 22.4 m^2 (g catalyst)$^{-1}$ for reduced catalyst.

Infrared spectra of discs at 295 K were recorded with a Perkin–Elmer 1720X FTIR spectrometer linked to a 7700 Computer. The resolution was 4 cm^{-1}. The spectra for CO on Cu often showed small shifts with changing conditions and band envelopes exhibited shoulders of varying intensity and clarity. However, the present condensed summary of the data is derived from a vast number of experiments involving different gas-phase pressures, sequences of addition of gases, ratios of gas pressures, and desorption conditions. The results were completely reproducible in terms of both band positions which are given here and relative band intensities.

RESULTS

Adsorption of Carbon Monoxide

Alumina. Carbon monoxide was adsorbed on calcined and reduced alumina which had been pretreated using identical procedures to those adopted for calcined and reduced Cu/Al_2O_3. For calcined alumina at 295 K weak bands slowly appeared at 1650, 1480, 1435, 1270 and 1230 cm^{-1}. The results were similar for reduced alumina (Figs. 1a–1c) although the bands were more intense than for the calcined oxide. The surface species responsible for the bands were slowly desorbed by evacuation at ambient temperature (Fig. 1d) and completely desorbed at 473 K (Fig. 1e). The bands at 1650 and 1230 cm^{-1} may be ascribed (28–32) to the ν_a(OCO) and β(OH) vibrations of a surface hydrogen carbonate although it is debatable whether the band at 1480 (28–31) or at 1435 cm^{-1} (32) may be due to the corresponding ν_s (OCO) vibration. The band at 1435 cm^{-1} is also in the expected spectral region for the $\nu_a(CO_3)$ vibration of uncoordinated carbonate ions (30). The weak band at 1270 cm^{-1} together with a very weak band at 1710 cm^{-1} (Fig. 1c) may be ascribed to a bridging surface carbonate (29).

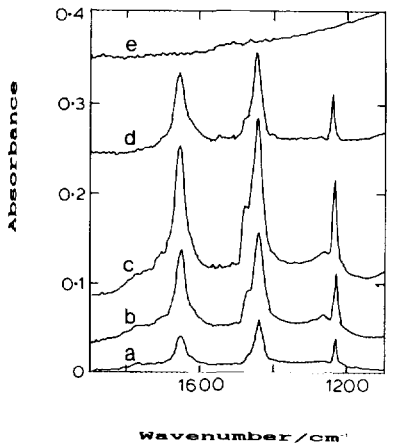

FIG. 1. Spectra of reduced alumina exposed at 295 K to CO (4 kN m^{-2}) for (a) ca. 1 min, (b) 30 min, (c) 120 min, followed by evacuation at (d) 295 K for 60 min, and (e) 473 K for 10 min.

Carbon monoxide generally is adsorbed to only very low maximum coverages on alumina surfaces via dative ligation to uncoordinated surface Al^{3+} cation sites giving infrared bands at ca. 2200–2245 cm^{-1} (33, 34). No such bands were observed here. However, in accordance with the present results, the formation of hydrogen carbonate from CO on alumina has been reported (35). Carbon dioxide may also be adsorbed on alumina (36) or boehmite (37) via either ligation to unsaturated surface cations or reaction with oxide or hydroxide ions to give carbonate or hydrogen carbonate species. The extreme weakness of the infrared bands observed here for CO on calcined alumina showed that the majority of the oxide surface would not adsorb CO (≤4 kN m^{-2}) at ambient temperature. Pretreatment in hydrogen at 483 K activated the surface for a higher level of CO oxidation to adsorbed hydrogen carbonate but failed to generate unsaturated Al^{3+} cations which could adsorb CO at ambient temperature. The enhanced ability of the surface to oxidise CO after reduction is reminiscent of related effects reported for the adsorption of acetone (38) and hexafluoroacetone (39) on rutile which had been pretreated at high temperature in hydrogen.

Calcined Cu/Al_2O_3. The addition of CO to calcined Cu/Al_2O_3 gave an infrared band envelope in the ν_{CO} spec-

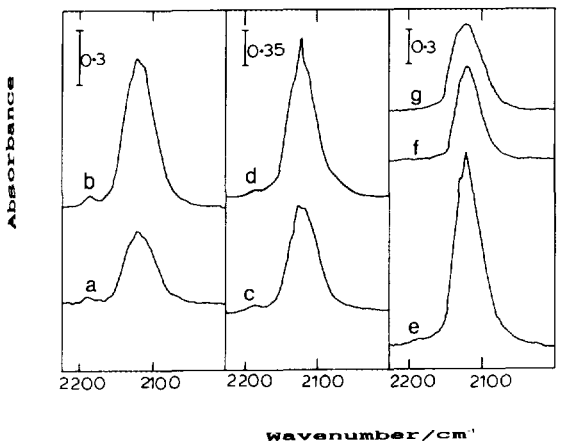

FIG. 2. Spectra of calcined Cu/Al_2O_3 exposed at 295 K to CO at (a) 0.27 kN m^{-2} (5 min), (b) 2.66 kN m^{-2} (5 min), (c) 4.00 kN m^{-2} (5 min), (d) 4.00 kN m^{-2} (90 min), (e) 4.00 kN m^{-2} (120 min), followed by (f) evacuation (295 K, 45 min), and then (g) evacuation (473 K, 10 min) and readmission of CO (295 K, 0.53 kN m^{-2}).

tral region with a maximum at 2122 cm^{-1}, shoulders at 2110 and 2133 cm^{-1}, and an additional weak band at 2191 cm^{-1} (Fig. 2a). The intensities of these bands increased with increasing pressure of carbon monoxide (Figs. 2b and 2c). However, there were also slow time-dependent effects which enhanced the intensity of the broad band envelope (Figs. 2d and 2e) (the final maximum was at 2120 cm^{-1} with shoulders at 2110 and 2128 cm^{-1}), but conversely weakened the band at 2192 cm^{-1}. Subsequent evacuation completely removed the latter band (<1 min) and after 45 min reduced the band envelope to ca. 50% of its initial intensity (Fig. 2f). Complete removal of adsorbed CO was achieved by evacuation at 473 K. Subsequent admission of CO gave a spectrum (Fig. 2g) which was similar to that for CO adsorption on freshly calcined Cu/Al_2O_3 although the low wavenumber shoulder appeared at 2102 cm^{-1}, a band position charcteristic of CO on Cu^0 (40). Some reduction to Cu^0 had probably occurred during removal of CO at 473 K. Alumina alone gave no bands in the ν_{CO} region in the presence of CO under the experimental conditions adopted here.

Calcined Cu/Al_2O_3 exposed to CO gave infrared bands in the 1800–1200 cm^{-1} spectral region which were characteristic of hydrogen carbonate on the alumina support. However, the bands appeared more rapidly and became much more intense in the presence rather than the absence of copper. Oxidised copper promoted the formation of hydrogen carbonate from CO on alumina. Additional broad bands for calcined Cu/Al_2O_3, not observed for alumina alone, were recorded at ca. 1550 and ca. 1380 cm^{-1} and may have been due to surface carbonate species (41) ligated to copper sites in the catalyst surface. These species were more resistant to removal by evacuation at 295 K than the hydrogen carbonate on alumina and were not completely desorbed even at 473 K.

Reduced Cu/Al_2O_3. Addition of carbon monoxide to reduced Cu/Al_2O_3 gave infrared bands in the range 1800–1200 cm^{-1} characteristic of CO adsorption on alumina alone. However, bands also appeared due to the nondissociative adsorption of CO on copper. Two dominant bands were at 2094 and 2087 (sh) cm^{-1} (Fig. 3a) shifting to 2099 and 2090 cm^{-1} (Fig. 3c) as the pressure of CO and hence surface coverage was increased. Weak shoulders were also present at 2140 and 2070 cm^{-1}, the latter particularly at high surface coverages. An additional very weak shoulder appeared at 2117 cm^{-1} after prolonged contact between CO and reduced Cu/Al_2O_3 at 295 K. The carbonyl species could be nearly entirely removed (<1% left) from the surface by evacuation at 295 K although species giving the bands at 2140 and 2117 cm^{-1} desorbed rather slowly. Readmission of CO at 295 K after a brief (10 min) evacuation at 473 K gave a spectrum similar to that for CO on freshly reduced Cu/Al_2O_3 showing that the CO adsorption/desorption experiment had not influenced the Cu surface in any irreversible way.

Carbon monoxide was adsorbed on reduced Cu/Al_2O_3 at much lower pressures than in the previous experiment in an attempt to identify the most active sites for CO adsorption. A gaseous mixture of 0.5% CO in argon was used to dose the CO into the infrared cell. The dominant band at the lowest CO pressure was at 2140 cm^{-1} with weaker maxima at 2125 and 2100 cm^{-1} (Fig. 3d). However, the band at 2140 cm^{-1} did not increase much further in intensity with increasing CO pressure, whereas the band at 2100 cm^{-1} grew until it became the dominant maximum

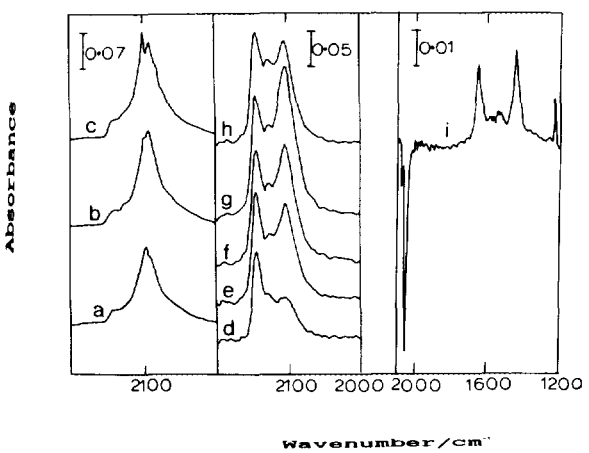

FIG. 3. Spectra of reduced Cu/Al_2O_3 exposed at 295 K to CO at (a) 0.27 kN m^{-2}, (b) 0.80 kN m^{-2}, and (c) 4.00 kN m^{-2}. Further disc with CO at pressures of (d) 1.35 N m^{-2} (e) 2.65 N m^{-2} (f) 4.00 N m^{-2}, (g) 5.30 N m^{-2} (all recorded after 5 min contact) and (h) 5.30 N m^{-2} (1 h contact). (i) Difference spectrum (h)–(g).

(Fig. 3g). There was also a time-dependent effect whereby the band at 2100 cm^{-1} in particular underwent a reduction in intensity which was accompanied by the concomitant appearance of infrared bands ascribed to hydrogen carbonate species on alumina (Figs. 3h and 3i).

Cu/Al_2O_3 (ex. N_2O). The decomposition of N_2O on Cu^0 gives $N_2(g)$ and a surface stoichiometry of $Cu^+O^{2-}Cu^+$. The modified surface therefore enables interactions between CO and Cu^+ sites to be characterised. Carbonyl complexes of copper initially gave bands at 2110 and 2132(sh) cm^{-1} (Fig. 4a). In addition a new band at 2098 cm^{-1} slowly grew with time up to 15 min when it attained its maximum intensity (Fig. 4b). Bands due to hydrogen carbonate species on alumina also grew with time, the rate of growth being faster than for CO on reduced Cu/Al_2O_3 for the first 15 min contact but with the rate being slower and equal to that for reduced Cu/Al_2O_3 after 15 min. The results imply that reduction of Cu^+ sites to Cu^0 in the first 15 min of contact was accompanied by carbon dioxide formation which promoted the appearance of the adsorbed hydrogen carbonate.

Evacuation at 295 K reduced the intensities of all bands in the ν_{CO} region, the effect being greatest for the maximum at 2098 cm^{-1} in accordance with the result for the desorption of CO from Cu^0 in reduced Cu/Al_2O_3. Comparison of the results for the three catalysts (calcined, reduced and ex. N_2O) shows that the ease of desorption of CO from surface sites was in the sequence Cu^{2+} > Cu^0 > Cu^+-in-a-Cu^+-environment > Cu^+-in-a-Cu^{2+}-environment. Readmission of CO to Cu/Al_2O_3 (ex N_2O) after evacuation at 295 K gave a spectrum (Fig. 4d) similar to that for fresh catalyst exposed to CO (Fig. 4a). However, after complete desorption of CO by evacuation at 473 K (Fig. 4e) and readmission of CO, the spectrum more closely resembled the result for CO on reduced Cu/Al_2O_3. Desorption of CO at 473 K and evacuation at 473 K had caused significant reduction of the partially oxidised surface.

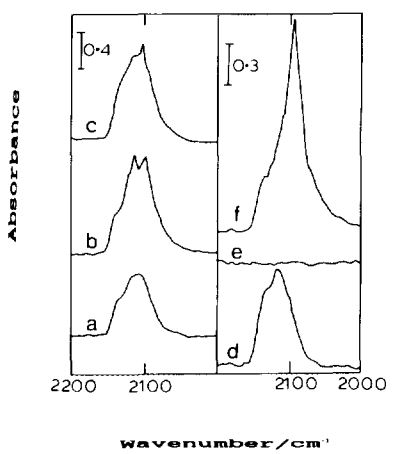

FIG. 4. Spectra of Cu/Al_2O_3 (ex. N_2O) exposed to CO at 295 K and 0.53 kN m^{-2} for (a) ca. 1 min, (b) 10 min, and (c) 120 min, (d) evacuated (295 K, 1 h) and CO (0.53 kN m^{-2}) readmitted, (e) evacuated (473 K, 10 min), and (f) CO (0.53 kN m^{-2}) readmitted.

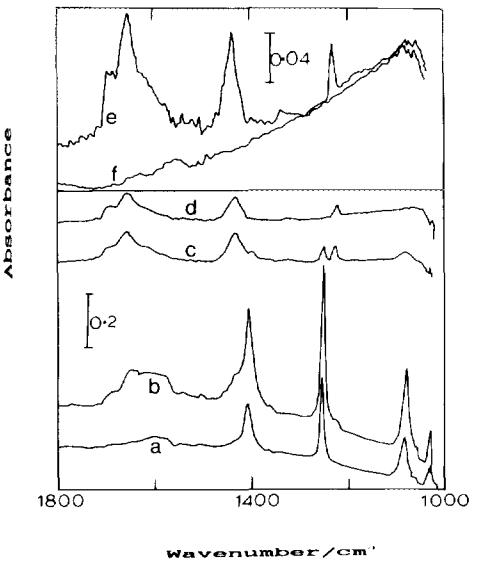

FIG. 5. Spectra of reduced alumina at 295 K exposed to thiophene at (a) 0.27 kN m^{-2} and (b) 1.33 kN m^{-2}, before evacuation at 295 K for (c) 1 min, (d) 15 min, and (e) 60 min, and (f) further evacuation (473 K, 20 min).

Adsorption of Thiophene

Alumina. The initial stage of adsorption of thiophene on reduced alumina gave infrared bands at 1600, 1406, 1362 (vw), 1253, 1082, and 1032 cm^{-1} (Fig. 5a) which resemble similar bands in the spectrum of liquid thiophene. At higher contact pressures of thiophene weak bands also appeared at 1685, 1650, 1435 (sh), and 1230 cm^{-1} (Fig. 5b). The latter three bands may be ascribed to hydrogen carbonate species which were resistant to desorption by evacuation at 295 K (Figs. 5d and 5e) but were removed at 473 K (Fig. 5f). Reduction of titanium dioxide in hydrogen is known to promote surface oxidation of adsorbed organic molecules (38, 39). The present result would be compatible with a similar effect for a small number of surface sites on alumina. Nondissociatively adsorbed thiophene molecules were rapidly desorbed by evacuation at 295 K (Figs. 5c and 5d).

The present sample of alumina scattered radiation badly in the range 4000–2500 cm^{-1} and therefore meaningful spectra in this spectral region could not be recorded. Brief experiments were carried out with Degussa grade C γ-Al_2O_3 (area 150 m^2 g^{-1}) which scattered radiation to a much lesser extent. The two samples of alumina gave identical results in the 1800–1000 cm^{-1} region for the adsorption of thiophene although the appearance of bands due to hydrogen carbonate did not occur for the Degussa

alumina. However, the latter was evacuated at 873 K (2 h) and not subjected to reduction in hydrogen before exposure to thiophene. The reduction process promoted the generation of hydrogen carbonate from CO and therefore it appears that a related promotional effect occurred during thiophene adsorption.

The Degussa alumina was preheated at 873 K in order to be able to monitor clearly the behaviour of surface hydroxyl groups in the presence of thiophene. The hydroxyl groups gave infrared bands at 3794, 3735, and 3707 cm^{-1}. Decreases in the intensities of these bands with increasing admitted pressure of thiophene were accompanied by the concomitant appearance of a broad maximum at 3582 cm^{-1}. These effects were reversed by evacuation at 295 K showing that adsorption involved the formation of hydrogen bonds between surface hydroxyl groups and thiophene molecules. Adsorbed thiophene also gave infrared bands due to CH-stretching vibrations at 3110 and 3077 cm^{-1}, band positions closely similar to those for liquid thiophene. However, additional weak bands also appeared at 2981 and 2965 cm^{-1} and may be assigned to CH-stretching vibrations of saturated alkyl species. The adsorption of thiophene on a fully deuterated alumina surface also led to the appearance of bands at 2981 and 2965 cm^{-1} with no bands which might be assigned to CO-stretching vibrations. This result implies, contrary to a previous suggestion (42), that the saturated alkyl species were not generated by transfer to thiophene of hydrogen atoms from surface hydroxyl groups. Similar saturated alkyl species have been reported for thiophene adsorbed on silica or reduced Cu/SiO_2 (26, 43), although the exact nature of the species remains in doubt (44). In the present context it appears unlikely that these products of thiophene adsorption on silica or alumina influence the behaviour of thiophene on the copper component of Cu/SiO_2 and Cu/Al_2O_3 catalysts. Proof of this surmise would require an infrared study of thiophene and CO adsorption on unsupported copper. Results for thiophene alone are compatible with the present conclusions (20).

Calcined Cu/Al_2O_3. The adsorption of thiophene on calcined Cu/Al_2O_3 gave an infrared spectrum (Fig. 6a) which was primarily characteristic of thiophene on calcined alumina. However, weak additional bands were detected at 1397 (sh), 1312, and 1218 cm^{-1} when copper was present and are assigned to thiophene molecules interacting with the Cu^{2+} surface sites via their π electrons (45). Carbon monoxide was then added as a probe molecule to test the effects of thiophene adsorption on surface sites. A band envelope due to linearly adsorbed CO had a maximum at 2113 cm^{-1} and a shoulder at 2130 cm^{-1} (Fig. 6c). The intensity of the band envelope was about the same as that of the envelope with a maximum at 2122 cm^{-1} for CO on calcined Cu/Al_2O_3 in the absence

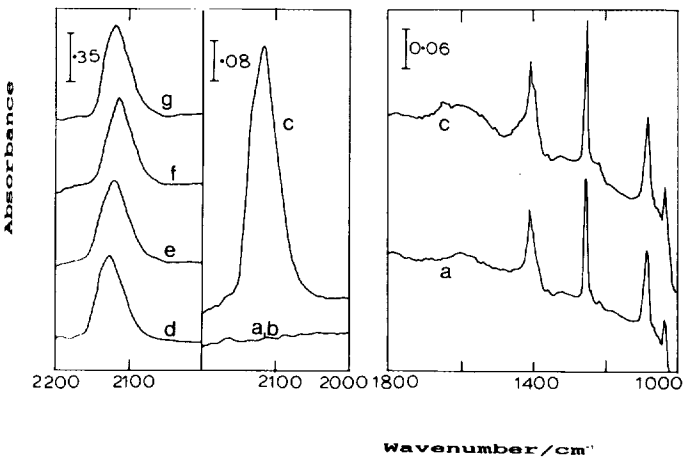

FIG. 6. Spectra of calcined Cu/Al_2O_3 at 295 K exposed to (a) thiophene (0.27 kN m^{-2}), (b) thiophene (0.53 kN m^{-2}), and (c) thiophene (0.53 kN m^{-2}) + CO (0.53 kN m^{-2}). Further sample exposed to (d) CO (0.53 kN m^{-2}), (e), (f) CO (0.53 kN m^{-2}) + thiophene at (e) 0.27 kN m^{-2}, (f) 1.33 kN m^{-2}, followed by (g) evacuation (295 K).

of thiophene. The band shift induced by co-adsorption of thiophene occurred with the absence (Fig. 6c) of the weak band at 2191 cm^{-1} observed when thiophene was not present (Fig. 2). The addition of CO did not affect the spectrum of adsorbed thiophene in the 1800–1200 cm^{-1} spectral region although weak bands characteristic of CO on calcined alumina did appear (Fig. 6c).

The addition of thiophene to calcined Cu/Al_2O_3 after the preaddition of CO shifted the bands for CO alone (2122, 2110 (sh), 2133 (sh)) to 2113 and 2130 (sh) cm^{-1} and removed the weak maximum at 2191 cm^{-1} (Figs. 6d and 6e). The intensity of the band envelope due to ν_{CO} vibrations was insensitive to the presence of thiophene, to thiophene pressure (Fig. 6f), or to time of contact (<2 h) at 295 K. The bands at 1397 (sh), 1312, and 1218 cm^{-1} due to thiophene interacting with Cu^{2+} sites were also observed when thiophene was added after CO to the catalyst. Otherwise the lower spectral region was again characteristic of thiophene and CO on alumina. Subsequent evacuation at 295 K rapidly (>90% in ≤1 min) desorbed thiophene from alumina. At the same time the ν_{CO} vibrations of CO on copper reverted to give bands at 2122 and 2133 (sh) cm^{-1} (Fig. 6g). Weak bands due to thiophene on Cu^{2+} sites became weaker but were still detectable in spectra even after 1 h evacuation. The desorption of CO was consistent with the result for a surface untreated with thiophene (Fig. 2), although comparison of band intensities as a function of time showed that CO was slightly more strongly adsorbed on catalysts which had been treated with thiophene. Subsequent attempts to completely desorb material from the surface involved heat treatment at 473 K in vacuum. A series of infrared bands remained and could probably be ascribed to carboxylate species on alumina. Despite this, the addition of CO gener-

ated a typical ν_{CO} spectrum for CO on freshly calcined Cu/Al_2O_3 except that the band at 2191 cm^{-1} was absent, suggesting that the copper surface had been freed from the effects of thiophene except for the sites giving the maximum at 2191 cm^{-1} in the presence of CO on an unmodified surface.

Reduced Cu/Al_2O_3. Results in the 1800–1200 cm^{-1} spectral region for thiophene adsorption with and without addition of CO as a probe molecule could largely be attributed to typical adsorption behaviour of thiophene or CO on reduced alumina. The only exceptions were the appearance of additional bands at 1588 cm^{-1}, previously attributed to thiophene coordinated to unsaturated Al^{3+} sites (46) and 1372 and 1191 cm^{-1}, attributed to thiophene adsorbed on zerovalent copper (18).

The addition of carbon monoxide to reduced Cu/Al_2O_3 pretreated with thiophene gave a ν_{CO} band envelope which more closely resembled the result for CO adsorption on Cu/Al_2O_3 (ex N_2O) than that for reduced Cu/Al_2O_3 (Fig. 7b). The maximum was at 2116 cm^{-1} with just discernible shoulders at 2134 and 2094 cm^{-1}. Figures 7c–7f show the result of a reverse experiment in which CO was added before thiophene. Exposure to thiophene resulted in the disappearance of the maximum at 2094 cm^{-1} due to CO on Cu^0 and the appearance of the bands due to CO on partially oxidised copper. The intensities of the latter bands were enhanced as increasing pressures of thiophene were admitted to the infrared cell. After prolonged reaction (Fig. 7g) the spectral maximum was at 2110 cm^{-1} with a shoulder at 2098 cm^{-1}. This result resembles that in Fig. 4b although there the band at 2098 cm^{-1} was more intense than that at 2110 cm^{-1}.

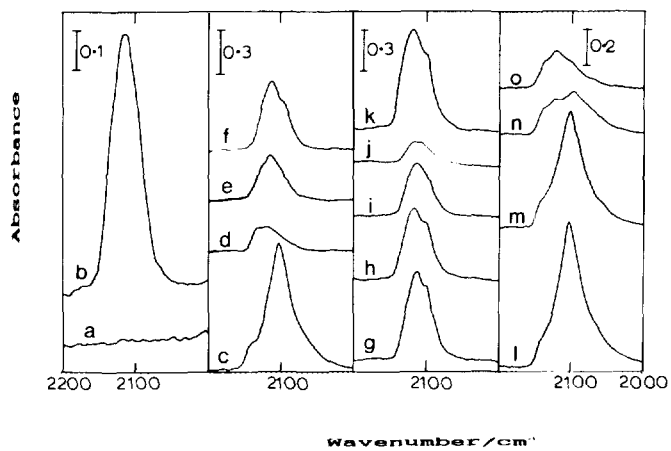

FIG. 7. Spectra of reduced Cu/Al_2O_3 at 295 K (a) exposed to thiophene (0.27 kN m^{-2}, 30 min), followed by (b) (0.53 kN m^{-2}, 10 min); (c) exposed to CO (0.53 kN m^{-2}) followed by (each for 20 min) (d) 0.27 kN m^{-2} (e) 0.80 kN m^{-2} (f) 1.33 kN m^{-2} thiophene, and (g) 120 min exposure at 1.33 kN m^{-2}. (h)–(j) Subsequent evacuation for (h) 1 min, (i) 5 min, and (j) 60 min, before (k) readmission of CO (0.53 kN m^{-2}) (l) exposed to CO (0.53 kN m^{-2}), followed by thiophene (9.3 N m^{-2}) and left to stand for (m) 5 min (n) 10 min, and (o) 20 min.

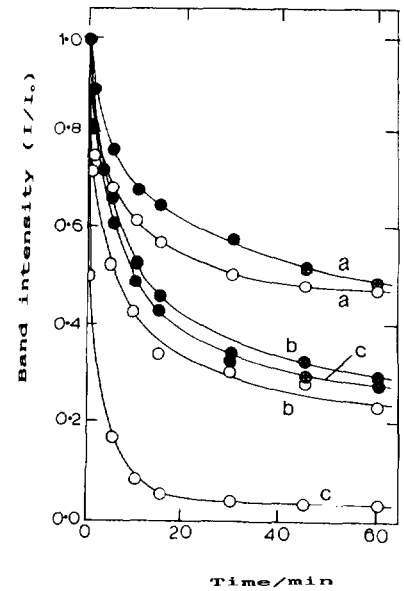

FIG. 8. Decrease with time of evacuation at 295 K of band maximum intensity I (normalised to unity for the initial intensity I_0) for CO adsorbed on (a) calcined Cu/Al_2O_3, (b) Cu/Al_2O_3 (ex. N_2O), and (c) reduced Cu/Al_2O_3. Open and closed circles denote without and with thiophene treatment, respectively.

Adsorbed CO was slowly desorbed from the thiophene-treated reduced Cu/Al_2O_3 surface by evacuation (Figs. 7h–7j). The ease of removal of CO from this catalyst resembled the corresponding result for CO desorption from Cu/Al_2O_3 (ex. N_2O) (Fig. 8). Carbon monoxide was much more easily desorbed from untreated reduced Cu/Al_2O_3. After a large proportion of the CO had been desorbed (Fig. 7g), CO was readmitted. The resulting spectrum was similar to that before desorption showing that the effects of thiophene treatment had been retained by the surface after thiophene and CO had been removed from the gas phase.

Reduced Cu/Al_2O_3 was exposed to CO and the time-dependent effects of the subsequent addition of a low pressure of thiophene were monitored (Figs. 7l–7o). The spectrum before the addition of thiophene contained bands at 2094, 2070(sh), and 2140(sh) cm^{-1} (Fig. 7l); after the addition of thiophene the intensities of the bands at 2094 and 2070 (sh) cm^{-1} declined and a new band appeared at 2120 cm^{-1} (Fig. 7n). There was also evidence for a new shoulder at 2102 cm^{-1} (Fig. 7o). The shoulder at 2140 cm^{-1} appeared insensitive to the addition of thiophene. Further additions of thiophene to the system resulted in a band maximum shift from 2120 to 2116 cm^{-1} and a shift of the shoulder at 2102 cm^{-1} to 2094 cm^{-1}.

Cu/Al_2O_3 (ex. N_2O). Spectra in the 1800–1200 cm^{-1} region of coadsorbed CO and thiophene on Cu/Al_2O_3 (ex. N_2O) showed no features other than those characteristic of the separate adsorption of CO and thiophene. The adsorption of thiophene followed by CO gave ν_{CO} bands at

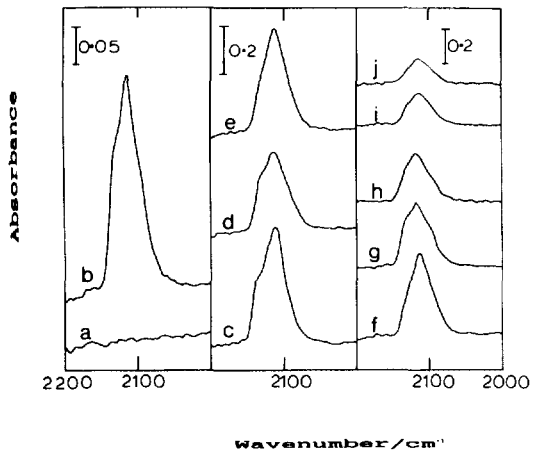

FIG. 9. Spectra of Cu/Al_2O_3 (ex. N_2O) exposed at 295 K to (a) thiophene (0.53 kN m^{-2}), followed by (b) CO (0.53 kN m^{-2}). Further disc exposed to (c) CO (0.53 kN m^{-2}), followed by thiophene at (d) 0.27 kN m^{-2}, (e) 1.06 kN m^{-2}, and (f) 1.33 kN m^{-2}, with subsequent evacuation at 295 K for (g) 1 min, (h) 5 min, (i) 15 min, and (j) 60 min.

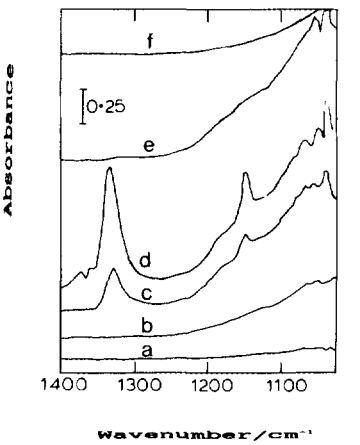

FIG. 10. Spectra of calcined alumina exposed to SO_2 at 295 K and (a) 13.5 N m^{-2}, (b) 53 N m^{-2}, (c) 319 N m^{-2}, and (d) 851 N m^{-2}, followed by evacuation at (e) 295 K (15 min) and (f) 473 K (10 min).

2115 and 2132 (sh) cm^{-1} (Fig. 9b). In reverse experiments (Figs. 9c–9f) the band maximum at 2110 cm^{-1} due to CO alone on the catalyst was shifted to 2115 cm^{-1} after the subsequent addition of thiophene. Carbon monoxide could be partially desorbed from the thiophene-treated catalyst by evacuation at 295 K (Figs. 9g–9j). Quantitative comparisons of the loss of absorption intensity at 2115 cm^{-1} with time (Fig. 8) showed that the ease of desorption of CO from thiophene-treated Cu/Al_2O_3 (ex. N_2O) was similar to that for both untreated Cu/Al_2O_3 (ex. N_2O) and reduced Cu/Al_2O_3 which had been treated with thiophene.

Adsorption of Sulphur Dioxide

Alumina. Similar spectra were observed for calcined alumina and reduced alumina in contact with sulphur dioxide. The addition of SO_2 to alumina initially gave a broad band at ca. 1050 cm^{-1} which may be ascribed to a unidentate sulphur-bound sulphite species (47) and weak broad shoulders at 1125 and 1180 cm^{-1} (Fig. 10b) which have been attributed to SO_2 ligated to unsaturated oxygen and aluminium ions, respectively (47). The dominant infrared bands at 1335 and 1149 cm^{-1} (Figs. 10c and 10d) appeared at high pressures of SO_2 and may be assigned to the $\nu_{as}(SO_2)$ and $\nu_s(SO_2)$ vibrations of SO_2 molecules physically adsorbed on surface hydroxyl groups (47–50) which led to a concomitant decline in the intensities of infrared bands due to hydroxyl groups (47, 48, 50). Bands at 1374 and 1360 cm^{-1} (Fig. 10d) were due to vibrations of gas-phase SO_2.

Physically adsorbed SO_2 was rapidly desorbed by evacuation at 295 K (Fig. 1e) but the more strongly adsorbed species giving bands at 1050, 1125 (vw), and 1180 (vw) cm^{-1} were partially retained (Fig. 10e). The latter species had disappeared after evacuation at 473 K (Fig. 10f).

Calcined Cu/Al_2O_3. Treatment of calcined Cu/Al_2O_3 with SO_2 at 295 K gave infrared spectra which were identical to the corresponding result for calcined alumina alone. There were no additional bands which could be ascribed to adsorbed species resulting from interactions between SO_2 and the copper component of the catalyst. However, spectra of subsequently adsorbed CO showed that exposure to SO_2 had influenced the adsorptive properties of oxidised copper. The admission of CO gave a single ν_{CO} infrared band at 2131 cm^{-1} (Fig. 11b). This band was narrower than the ν_{CO} band envelope for adsorbed CO in the absence of SO_2 and in particular did not show a shoulder at 2110 cm^{-1} or an additional weak band at 2191 cm^{-1}. Furthermore no bands due to hydrogen carbonate or carbonate species on alumina were observed in contrast to the result for CO adsorption on calcined Cu/Al_2O_3 in the absence of SO_2.

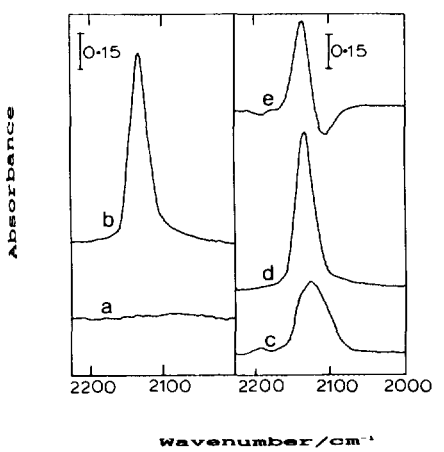

FIG. 11. Spectra of calcined Cu/Al_2O_3 exposed at 295 K to (a) SO_2 (270 N m^{-2}) and (b) SO_2 (270 N m^{-2}) + CO (530 N m^{-2}). Further sample exposed to (c) CO (530 N m^{-2}) and (d) CO (530 N m^{-2}) + SO_2 (530 N m^{-2}). (e) Difference spectrum (d)–(c).

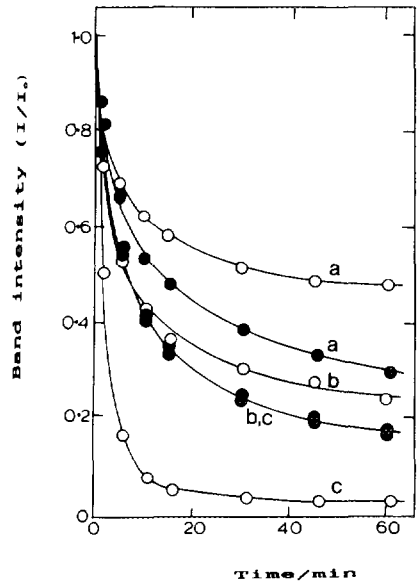

FIG. 12. Decrease with time of evacuation at 295 K of band maximum intensity I (normalised to unity for the initial intensity I_0) for CO adsorbed on (a) calcined Cu/Al_2O_3, (b) Cu/Al_2O_3 (ex. N_2O), and (c) reduced Cu/Al_2O_3. Open and closed circles denote without and with sulphur dioxide treatment, respectively.

Experiments in which CO was added before SO_2 to calcined Cu/Al_2O_3 confirmed the effects of SO_2 on surface sites for the adsorption of CO. Carbon monoxide adsorption gave infrared bands at 2191, 2133 (sh), 2122, and 2110 cm^{-1} (Fig. 11c). Subsequent addition of SO_2 resulted in the disappearance of the weak band at 2191 cm^{-1} (Fig. 11d) due to CO ligated to isolated Cu^{2+} surface sites (51, 52). The main band maximum shifted from 2122 to 2131 cm^{-1}. Difference spectra (Fig. 11e) showed that the shift resulted from loss of absorption intensity at 2104 cm^{-1} and the growth of a band at 2134 cm^{-1}. Further additions of CO up to 1.33 kN m^{-2} had no effect on the ν_{CO} band shape although the intensity increased by ca. 16%. Spectra in the 1800–1000 cm^{-1} region were similar to those for SO_2 adsorbed on calcined Cu/Al_2O_3 which had not been exposed to CO.

Evacuation at 295 K caused the slow removal of adsorbed CO from calcined Cu/Al_2O_3 which had been exposed to SO_2. Comparison of the loss of band maximum intensity as a function of time for untreated and SO_2-treated catalysts (Fig. 12a) suggested that adsorption of SO_2 weakened the subsequent adsorption of CO which was therefore easier to desorb by evacuation. Evacuation also completely removed physically adsorbed SO_2 from the alumina surface. However, readmission of CO regenerated the single narrow band maximum at 2131 cm^{-1} rather than the typical spectrum in the ν_{CO} region for CO on untreated catalyst. The effects of the SO_2 adsorption on copper sites for adsorption of CO were therefore not reversed by removal of gas-phase SO_2 at 295 K. Furthermore, evacuation at 473 K followed by readmission of CO also gave the characteristic ν_{CO} band for SO_2-treated catalyst.

Reduced Cu/Al_2O_3. Bands in the 1800–1000 cm^{-1} spectral region for reduced Cu/Al_2O_3 exposed to SO_2 were identical to the bands resulting from SO_2 adsorption on alumina alone. There were no detectable features attributable to surface species on copper. In contrast to the result for reduced Cu/Al_2O_3 which had not been exposed to SO_2, subsequent exposure to CO failed to generate surface hydrogen carbonate or carbonate species on alumina, showing that CO adsorption on the support was inhibited by SO_2 adsorption. The spectrum of CO on copper sites gave a single band at 2124 cm^{-1} (Fig. 13b) for SO_2-treated catalyst. This result differs significantly from the corresponding result for reduced Cu/Al_2O_3 which had not been exposed to SO_2, showing indirectly that SO_2 was being adsorbed on the copper component of the catalyst.

In a reverse experiment CO was initially added to reduced Cu/Al_2O_3, giving ν_{CO} bands at 2140 (sh), 2094, and 2070 (sh) cm^{-1} (Fig. 13c). Subsequent admission of SO_2 caused a slow transformation in the spectrum resulting in a band maximum shift to 2124 cm^{-1} (Figs. 13b–13e). A difference spectrum (Fig. 13f) showed that the total change involved the loss of bands at 2094 and 2070 (sh) cm^{-1} due to CO adsorbed on Cu^0 sites and the appearance of bands at 2124 and ca. 2150 cm^{-1} due to CO on Cu^+ sites in two different environments. Further increase in SO_2 pressure (<1.33 kN m^{-2}) did not alter the shape of the ν_{CO} band envelope although the band intensity was increased to 157% of its value in the difference (Fig. 13f). Adsorbed CO on Cu^+ sites was slowly desorbed by evacuation at 295 K (Figs. 13h–13k). However, readmission of

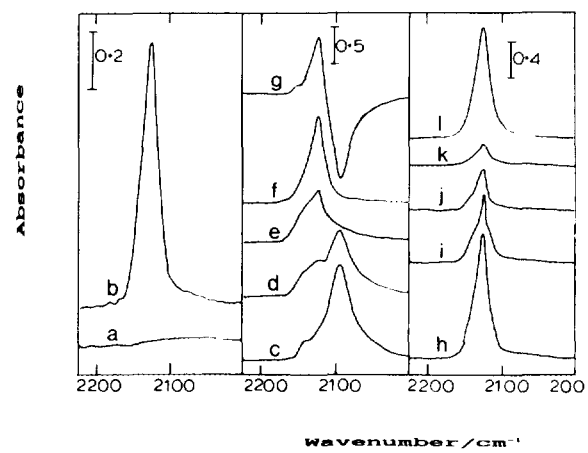

FIG. 13. Spectra of reduced Cu/Al_2O_3 at 295 K (a) exposed to SO_2 (270 N m^{-2}) followed by (b) CO (530 N m^{-2}); (c) exposed to CO (530 N m^{-2}) followed by (d)–(f) SO_2 (270 N m^{-2}) for (d) ca. 1 min, (e) 5 min, and (f) 20 min. (g) Difference spectrum (f)–(c). (h) Spectra exposed to CO (530 N m^{-2}) + SO_2 (1.33 kN m^{-2}) followed by evacuation (295 K) for (i) 5 min, (j) 15 min, and (k) 60 min, and subsequently (l) readmission of CO (530 N m^{-2}).

CO regenerated the band maximum at 2124 cm^{-1} (Fig. 13l), showing that the effects of adsorption of SO_2 at 295 K were not reversed by evacuation at 295 K. Adsorbed CO was more difficult to desorb from SO_2-treated reduced Cu/Al_2O_3 than from reduced Cu/Al_2O_3 which had not been treated with SO_2 (Fig. 12c).

In an attempt to gain more detailed information about the effect of SO_2 on copper sites, a reduced Cu/Al_2O_3 disc was exposed to CO followed by a low pressure of SO_2. Slow interaction of the SO_2 with the Cu^0 surface resulted in decreases in the intensities of the bands at 2094 and 2070 (sh) cm^{-1} due to CO on Cu^0 and growth of a maximum at 2120 cm^{-1} due to CO on Cu^+ sites (Figs. 14a–14e). After ca. 3 h reaction no further change in the spectrum occurred and therefore a further amount of SO_2 was added. The band at 2120 cm^{-1} then continued to grow at the expense of the maximum at 2098 cm^{-1} (Figs. 14e–14j). Again the spectrum became stable after ca. 3 h and a further aliquot of SO_2 was added (Figs. 14j–14l). The final spectrum after SO_2-induced changes were complete a narrow maximum at 2120 cm^{-1} with a scarcely discernible shoulder at 2140 cm^{-1} (Fig. 14l).

A question which arises is whether the pre-adsorption of CO in the above experiment impeded the interaction between SO_2 and copper, thus accounting for the long equilibration times. Reduced Cu/Al_2O_3 was exposed to a low pressure of SO_2 (cf. Figs. 14f–14j) for 5 min, evacuated for 20 min, and exposed to CO. The resulting spectrum (Fig. 14n) showed that considerably more change resulting from SO_2 treatment had occurred than after 5 min contact with SO_2 after adsorption of CO and closely resembled the final spectrum after 3 h contact (Fig. 14j)

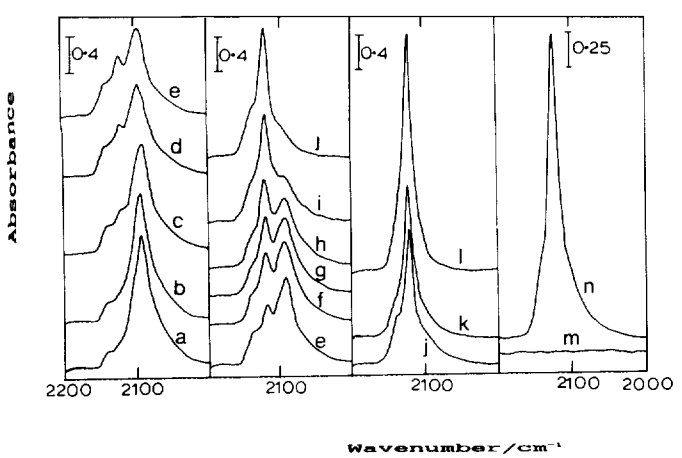

FIG. 14. Spectra of reduced Cu/Al_2O_3 exposed to (a) CO (530 N m^{-2}), and then CO (530 N m^{-2}) + SO_2 (13.3 N m^{-2}) for (b) ca. 1 min, (c) 15 min, (d) 90 min, and (e) 180 min, and then CO (530 N m^{-2}) + SO_2 (26.6 N m^{-2}) for (f) ca. 1 min, (g) 10 min, (h) 15 min, (i) 45 min, and (j) 180 min, and then CO (530 N m^{-2}) + SO_2 (40 N m^{-2}) for (k) ca. 1 min and (l) 90 min. (m) Further disc exposed to SO_2 (26.6 N m^{-2}) for 5 min and evacuated (295 K, 20 min) before (n) admission of CO (530 N m^{-2}).

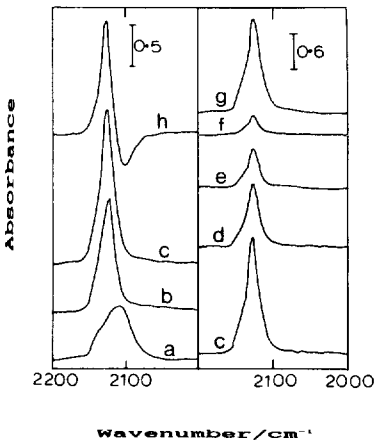

FIG. 15. Spectra of Cu/Al_2O_3 (ex. N_2O) exposed to (a) CO (530 N m^{-2}) followed by SO_2 at (b) 0.27 kN m^{-2} and (c) 1.33 kN m^{-2} (20 min), followed by evacuation at 295 K for (d) 5 min, (e) 15 min, (f) 60 min, and then (g) readmission of CO (530 N m^{-2}). (h) Difference spectrum (c)–(a).

when CO was also present. Adsorbed CO clearly impeded the reaction of SO_2 with the copper surface.

Cu/Al_2O_3 (ex. N_2O). Adsorption of CO on Cu/Al_2O_3 (ex. N_2O) gave ν_{CO} bands at 2110 and 2132 (sh) cm^{-1} due to CO adsorbed on Cu^+ in two different environments and a weak shoulder at 2098 cm^{-1} due to CO on Cu^0 sites generated by surface reduction of Cu^+ to Cu^0 by CO (Fig. 15a). Subsequent addition of SO_2 shifted the band maximum from 2110 to 2125 cm^{-1} with a weak shoulder to higher wavenumber (Figs. 15b and 15c). A difference spectrum (Fig. 15h) showed that loss of the bands and 2110 and 2098 (sh) was accompanied by the growth of a narrow maximum at 2125 cm^{-1}. Carbon monoxide was slowly desorbed from the SO_2-treated catalyst by evacuation at 295 K (Figs. 15d–15f). The ease of desorption of CO from SO_2-treated Cu/Al_2O_3 (ex. N_2O) was nearly identical to the ease of desorption from reduced Cu/Al_2O_3 which had been treated with SO_2 (Fig. 12). Subsequent readmission of CO (Fig. 15g) regenerated the band maximum at 2125 cm^{-1}, showing that the effects of SO_2 adsorption on Cu/Al_2O_3 (ex. N_2) were not reversed by evacuation at 295 K. The result in Fig. 13n is also consistent with this conclusion. There were no bands in the the 1800–1000 cm^{-1} spectral region which could be ascribed to SO_2 species on copper in Cu/Al_2O_3 (ex. N_2O). However, the addition of SO_2 impeded the subsequent generation of hydrogen carbonate from interaction between CO and the alumina support.

DISCUSSION

Table 1 gives a summary of the ν_{CO} band positions for three types of Cu/Al_2O_3 catalyst exposed to CO either before or after exposure to thiophene or SO_2. Figures 8 and 12 compare the relative ease of desorption of CO at

TABLE 1

Infrared Band Positions (ν_{CO}/cm^{-1}) for CO on Cu/Al_2O_3 Catalysts either Untreated with an S-Compound or with Coadsorbed Thiophene or Sulphur Dioxide

Catalyst	Co-adsorbate	ν_{CO} (cm^{-1})							
Calcined	None	2191	2133 (sh)	2122		2110 (sh)			
Calcined	Thiophene		2130 (sh)		2113				
Calcined	Sulphur dioxide		2131						
Ex. N_2O	None		2132 (sh)			2110	2098		
Ex. N_2O	Thiophene		2132 (sh)		2115				
Ex. N_2O	Sulphur dioxide			2125					
Reduced	None		2140				2099, 2090 (sh), 2070 (sh)		
Reduced	Thiophene		2134 (sh)		2116		2094 (sh)		
Reduced	Thiophene		2134 (sh)			2110	2098 (sh)		
Reduced	Sulphur dioxide		2140 (sh)	2124					
Adsorption sites		Cu^{2+}	Cu^+	Cu^+	Cu^+	Cu^+	Cu^0	Cu^0	Cu^0

595 K from catalysts with and without coadsorption of thiophene or SO_2 with CO.

CO Adsorption on Calcined Cu/Al_2O_3

The band at 2191 cm^{-1} for CO on calcined Cu/Al_2O_3 is like a similar band for a copper(II) zeolite (51) and is indicative of CO ligated to Cu^{2+} surface sites (52). The band was not observed for CO adsorption on copper(II) oxide (41, 53) suggesting that it was due to CO bound to a Cu^{2+} site isolated in the alumina support matrix (54).

Bands at 2133 (sh), 2122, and 2110 (sh) for CO on calcined Cu/Al_2O_3 may be ascribed to CO ligated to Cu^+ surface sites (41, 51, 52, 54, 55). The exact ν_{CO} band position is considered to be dependent on the environment of the Cu^+ ion to which the CO is bound. An increase from 2100 to 2140 cm^{-1} was suggested as indicating a greater concentration of Cu^{2+} ions in positions surrounding the Cu^+ adsorption site (53, 56). On this basis the shoulder at 2110 cm^{-1} (Table 1) would be attributable to CO on a Cu^+ site in a more reduced environment than that around the Cu^+ site adsorbing CO to give the band at 2133 cm^{-1}. The presence of at least three ν_{CO} bands suggests the presence of at least three different environments of Cu^+ ions on the surface of calcined Cu/Al_2O_3. The generation of Cu^+ sites would have occurred during the high-termperature (583 K) evacuation of catalyst after calcination and before exposure to CO (52–54, 57, 58).

With increasing pressures of CO, and in particular with longer contact times, the band envelope due to ν_{CO} bands showed enhanced intensity of the band at 2110 cm^{-1} relative to the bands at 2122 cm^{-1} and more particularly 2133 cm^{-1}. This implies that some CO-induced reduction of the oxidised surface copper cations ($Cu^{2+} \rightarrow Cu^+$) was slowly occurring, giving a higher preponderance of CO adsorption sites surrounded by Cu^+ rather than Cu^{2+} ions. Supporting this suggestion was the enhancing effect of oxidised copper on the formation of hydrogen carbonate species on the Al_2O_3 surface. Surface reduction by CO led to the formation of carbon dioxide which was subsequently chemisorbed on the alumina support. Surface reduction by CO also led to the appearance of additional infrared bands at 1550 and 1380 cm^{-1} ascribed to carbonate species on the copper component of the catalyst. Davydov (41) reported similar bands resulting from oxidation of CO to carbon dioxide and subsequent adsorption as carbonate on copper(II) oxide.

CO/Thiophene on Calcined Cu/Al_2O_3

The absence of the band at 2191 cm^{-1} for CO adsorbed on thiophene-treated calcined Cu/Al_2O_3 suggests that the adsorption of thiophene at isolated Cu^{2+} sites blocks the adsorption of CO at these sites. The downward shift of the dominant ν_{CO} band maximum from 2122 to 2113 cm^{-1} may be attributed to a lessening of the effect of Cu^{2+} cations in the vicinity of the Cu^+ sites on the adsorption of CO. Thiophene is adsorbed at Cu^{2+} sites, resulting in electron donation to the Cu^{2+} surface and thereby a strengthening of the interactions between CO and Cu^+ sites. The conclusion that thiophene (on Cu^{2+}) and CO (on Cu^+) are predominantly adsorbed on different but adjacent sites is consistent with the similar overall ν_{CO} band envelope intensities for the thiophene-treated and untreated catalyst. Thiophene does not impede CO adsorption but does influence the strength of interaction between CO and Cu^+ sites. This influence was reversed by evacuation at 295 K, showing that thiophene was desorbed from Cu^{2+} sites at 295 K but CO was retained at Cu^+ sites with a strength of adsorption similar to that for calcined Cu/Al_2O_3 which had not been treated with thiophene.

The infrared bands at 1397, 1312, and 1218 cm^{-1} for thiophene on calcined Cu/Al_2O_3 resemble bands pre-

viously reported (45) for thiophene adsorbed on a Cu^{2+}/montmorillonite. Cloos *et al.* (45) proposed the occurrence of electron donation from the π system of the thiophene ring to Cu^{2+} cations, an explanation which would be compatible with the present results. Electron transfer from a π electron system of adsorbate to copper(II) surface has also been suggested for benzene (59) and propene (60).

CO/SO$_2$ on Calcined Cu/Al$_2$O$_3$

The absence of a band at 2191 cm^{-1} for CO on calcined Cu/Al_2O_3 which had been exposed to SO_2 shows that the adsorption of SO_2 either displaces CO from isolated Cu^{2+} sites (51, 52) or poisons the sites for the subsequent adsorption of CO. Baxter *et al.* (22) reported the formation of a sulphite species on a copper(II) surface after exposure to SO_2 at ambient temperature. A unidentate O-bound sulphite complex would give infrared bands below 1000 cm^{-1} which would not have been detectable here because of the strong background absorption of the alumina support. Bands for unidentate S-bound species would be expected between 1130 and 1000 cm^{-1} (61). However, possible bands due to SO_3^{2-} species here would have been obscured by bands in the spectrum of SO_2 adsorbed on alumina and therefore the formation of sulphite species on oxidised copper is not precluded by the present data. Kent *et al.* (62) reported that sulphur dioxide was chemisorbed on copper(II) oxide and gave sulphite and sulphate species, one product of chemisorption involving ligation to copper sites via both S and O atoms. These results are in accord with the present observation that SO_2 blocks CO adsorption on Cu^{2+} sites.

Evacuation of calcined Cu/Al_2O_3 at 583 K for 1 h before the admission of adsorbate molecules causes partial reduction of the surface and the generation of Cu^+ sites. The dominant band maximum at 2122 cm^{-1} in spectra of calcined Cu/Al_2O_3 exposed CO is ascribed to CO ligated to Cu^+ sites in an environment containing both Cu^+ and Cu^{2+} vicinal sites (51–56). The exact ν(CO) band position is considered to be dependent on the environment of the Cu^+ ion to which the CO is bound. An increase from 2110 to 2140 cm^{-1} was suggested as indicating a greater concentration of Cu^{2+} ions in positions surrounding the Cu^+ adsorption site (51). The shift of the band to 2131 cm^{-1} for CO on sulphided calcined Cu/Al_2O_3 suggests a loss of electron density from vicinal sites (53, 56) via electron donation to adsorbed sulphur species. The easier removal of CO from Cu^+ sites on SO_2-treated rather than untreated catalyst supports this conclusion. Comparison of integrated band envelope intensities in Figs. 11c and 11d suggest that no Cu^+ sites available for CO adsorption were poisoned by the pre-adsorption of SO_2, although this conclusion requires the assumption that the extinction coefficient for CO on the SO_2-treated surface was not much greater than the extinction coefficient for CO on untreated calcined Cu/Al_2O_3. Overall there was a slight growth in absorption intensity (Fig. 11e) on exposure to SO_2. Thus, as for thiophene adsorption, it appears that SO_2 and CO are primarily adsorbed on different surface sites on oxidised copper but that the adsorption of CO influenced electronically by the adsorption of SO_2 on adjacent sites. Sulphur dioxide is predominantly adsorbed at Cu^{2+} cations and CO is predominantly adsorbed at exposed Cu^+ cations in the oxidised copper surface.

CO/Thiophene on Cu/Al$_2$O$_3$ (ex N$_2$O)

The dominant maximum at 2110 cm^{-1} for CO on Cu/Al_2O_3 (ex. N_2O) is as expected for CO on Cu^+ sites in a $Cu^+O^{2-}Cu^+$ environment (53, 56). The subsequent *in situ* reduction by CO of a limited proportion of Cu^+ sites to Cu^0 at 295 K has also been reported for Cu/SiO_2 (ex. N_2O) catalyst (63) treated in exactly the same way as the procedures adopted here for Cu/Al_2O_3. The present band at 2132 (sh) for Cu/Al_2O_3 (ex. N_2O), although weak, was present in spectra of adsorbed CO in all the spectra of thiophene-treated and untreated catalyst reported here (Table 1) and compares with a similar band 2125 cm^{-1} for untreated Cu/SiO_2 (ex. N_2O) (63). The latter was tentatively ascribed to CO on sites equivalent to those on high-index planes of Cu_2O.

The addition of thiophene to Cu/Al_2O_3 (ex. N_2O) gave an upward shift of 5 cm^{-1} in the ν_{CO} band position. The sulphur compound apparently induced electron transfer from the $Cu^+O^{2-}Cu^+$ surface to adsorbed thiophene molecules. By analogy, results for propene adsorption on copper catalysts led Efremov *et al.* (64) to propose that electron transfer from the catlayst surface to the π^* orbitals of propene had occurred. The enhanced cationic character of Cu^+ sites interacting with thiophene then gives an upward shift in the position of the infrared ν_{CO} band due to CO molecules co-adsorbed on adjacent Cu^+ sites, in accordance with the proposal that an increase in the band position (in cm^{-1}) reflects a higher degree of cationic character of Cu^{n+} ions adjacent to the Cu^+ CO-adsorption site (53, 56). The small decrease in absorption intensity of the ν_{CO} band in the presence of thiophene suggests that there may be some competition between CO and thiophene for a small proportion of the available adsorption sites. Otherwise thiophene adsorption has an electronic rather than a blocking effect on surface Cu^+ sites available for the adsorption of CO.

Coadsorption on Reduced Cu/Al$_2$O$_3$

Spectra of CO on reduced Cu/Al_2O_3 were in broad agreement with previous data (40, 54, 65–68). The main band maxima at 2087–2099 cm^{-1} are comparable with

bands for CO adsorbed on high-index single-crystal Cu^0 surfaces (40). The reduced Cu/Al_2O_3 apparently contained, as concluded before (40, 56, 69, 70), Cu^0 sites characteristic of corresponding sites in high-index planes of crystalline copper. The small coverage-dependent shifts to 2099 and 2090 cm^{-1} were similar to shifts for CO on single-crystal surfaces and are ascribed to the balancing of dipole–dipole coupling shifts with a changing electronic distribution (71, 72). The band at 2070 cm^{-1} is also ascribed to CO at Cu^0 sites, possibly similar to sites on low index planes of copper (63, 73). However, an alternative proposal is that the CO is bound to highly uncoordinated Cu^0 atoms, for example, at borderline (i.e., boundary) sites (56, 69, 70). The possible existence of Cu^+ ions at highly uncoordinated sites in reduced Cu/Al_2O_3 could account for the appearance of the weak ν_{CO} shoulder at 2140 cm^{-1} (70). In accordance both with this suggestion and with the desorption characteristics of CO from Cu^0 and Cu^+ sites (Fig. 8), the adsorption of CO at borderline Cu^+ sites in reduced Cu/Al_2O_3 was stronger than adsorption at Cu^0 sites in the same catalyst. Previous work has shown that CO adsorbs more strongly on Cu^+ than Cu^0 surface sites (70, 74, 75). The adsorption and desorption (Fig. 8) characteristics for CO on the present Cu/Al_2O_3 catalysts confirm that the strength of interaction between CO and copper adsorption sites is in decreasing order of strength Cu^+ (in a Cu^{2+} matrix) > Cu^+ (in a Cu^+ matrix) > Cu^0.

CO/Thiophene on Reduced Cu/Al_2O_3

The adsorption of CO on a thiophene-treated reduced Cu/Al_2O_3 catalyst was predominantly characteristic of CO on Cu^+ rather than Cu^0 sites. The sulphur compound induced electron transfer from surface copper atoms to adsorbed thiophene molecules. Similar electron transfer involving a metal surface and adsorbed sulphur species has been reported before (44, 76). Electron transfer between a Cu(110) surface and the π^* orbitals of adsorbed ethyne has also been observed (77). Molecular thiophene exists on copper at 300 K (19, 20). Thus electron transfer may occur from the copper surface to the sulphur atoms if thiophene rings are perpendicular to the copper surface. Alternatively, electron transfer from copper to the π^* orbitals of thiophene may occur if the thiophene rings are parallel to the surface.

The dramatic decline in ν_{CO} band intensity when thiophene was added (Fig. 7) suggests that thiophene was displacing and thence blocking sites for CO adsorption. However, the subsequent increase in ν_{CO} band intensity with increasing thiophene adsorption suggests that the mode of adsorption of thiophene was changing with increasing surface coverage. A plausible explanation is that thiophene rings lie parallel to the copper surface at low coverages thus blocking the access of CO to potential adsorption sites. As the pressure of thiophene is increased the orientation of the thiophene rings changes to being perpendicular to the surface and hence makes more of the surface sites accessible to CO molecules. This suggestion is in broad agreement with proposals of Sexton (20) who observed that the orientation of thiophene on a Cu(100) surface was pressure dependent. The present infrared bands at 1372 and 1191 cm^{-1} may be ascribed (20) to in-plane vibrations of intact thiophene rings, suggesting from the metal–surface selection rule that the rings are orientated perpendicular to the copper surface. The existence of thiophene parallel to the copper surface could not be confirmed since the out-of-plane vibrations which would confirm from the metal–surface selection rule, the existence of thiophene parallel to the copper surface, are below 1000 cm^{-1} (20). This low region could not be monitored because of intense absorption by the alumina support.

It would be of interest to use geometrical models of adsorption to test the present proposals for the co-adsorption of thiophene and CO on copper. However, this is unlikely to be profitable in the present context for very small clusters of copper atoms (ca. 15 Å particle diameter estimated from N_2O adsorption) because of uncertainties about particle shape and possible reconstruction effects on adsorption. Also such small clusters would have no exposed surfaces which would give properties typical of those expected for a well defined single crystal plane. One possibility would be that a high proportion of edge and apex sites in the particles and the close proximity of Cu atoms in different "faces" of the particles may favour electronic interactions between co-adsorbed thiophene and CO via copper atoms without imposing steric restrictions on their co-adsorption.

CO/SO_2 On Cu/Al_2O_3 (ex N_2O) and Reduced Cu/Al_2O_3

Despite the differences between the infrared data for CO adsorbed on Cu/Al_2O_3 (ex. N_2O) and reduced Cu/Al_2O_3 which had not been exposed to SO_2, the results for the two catalysts after treatment with SO_2 were nearly identical both from the point of view of band positions for ν_{CO} (Figs. 13b and 15c) and the ease of desorption of CO (Fig. 12). The upward $\Delta\nu_{CO}$ shift of 15 cm^{-1} for CO on SO_2-treated Cu/Al_2O_3 (ex. N_2O) (Table 1) suggests that the bonding of SO_2 to the partially oxidised copper surface involves electron transfer from the Cu(I) surface to adsorbed sulphur species. The Cu^+ sites for CO adsorption are therefore surrounded by a more electron-deficient environment than for catalyst in the absence of co-adsorbed SO_2 and this leads to weaker bonding between CO and the Cu^+ sites (53, 56). CO was more readily desorbed from SO_2-treated rather than untreated Cu/Al_2O_3 (ex. N_2O).

Oxidation of reduced Cu/ZnO in the presence of CO resulted in a shift in the ν_{CO} band from 2070 to 2140 cm^{-1} (56, 70). By analogy it may be proposed here that the present oxidative effect of SO_2 on the Cu^0 surface of reduced Cu/Al_2O_3 was to shift the bands at 2070 (sh) and 2094 cm^{-1} to 2140 (sh) and 2124 cm^{-1}, respectively. The two bands at 2140 and 2124 cm^{-1} for reduced Cu/Al_2O_3 treated with SO_2 and exposed to CO may therefore be due to copper sites either interacting with the same adsorbed sulphur species in different coordination geometries or interacting with different products of chemisorption of SO_2. The influence of electronic effects of one adsorbate on another has been demonstrated by Sárkány and Bartók (78, 74), who observed larger shifts in ν_{CO} as the electron donating power of a co-adsorbate was increased but the molecular size remained constant. The upward shift in ν_{CO} after SO_2 adsorption is hence indicative of electron transfer from the copper surface to the adsorbed species formed from SO_2. The changing electronic environment induces a greater donation of electrons from the 5σ orgital of CO to the copper adsorption sites and this causes the upward shift in ν_{CO} (80). Electron transfer is known to occur from metal sites to sulphur ad-atoms (44, 76, 81).

The present results do not support the contention that SO_2 does not adsorb on reduced copper at 298 K (21, 22) but are consistent with EELS results which suggested that SO_2 was chemisorbed at least on Cu(100) at 300 K (23). The proposed generation of sulphite by dissociative adsorption of SO_2 followed by reaction of further SO_2 with O ad-atoms would explain the similarity between the results for CO adsorption on reduced Cu/Al_2O_3 which had been exposed to SO_2 and on reduced Cu/Al_2O_3 which had been covered in O adatoms by pretreatment with N_2O. The band at 2124 cm^{-1} is therefore ascribed to CO adsorbed on Cu^+ sites which are influenced electronically by sulphite species at adjacent sites. The CO adsorption sites in their reduced state are equivalent to sites for CO adsorption in high-index planes of copper. The chemisorbed sulphur-containing species were unaffected by evacuation at 295 K since subsequent readmission of CO gave the characteristic spectrum for an SO_2-treated surface. Evacuation at 473 K followed by readmission of CO also gave a spectrum which was more typical of a partially oxidised surface which had been treated with SO_2 than a reduced surface, although the ν_{CO} band envelope was broader than that for reduced Cu/Al_2O_3 plus coadsorbed SO_2 and CO. High-temperature evacuation had not removed the effects of SO_2 adsorption but had changed their nature to some extent. In accordance with this result Leung *et al.* (23) suggested that sulphite species formed on copper at 300 K decomposed to adsorbed S and O adatoms at 350 K.

Recent results (43) for the co-adsorption of SO_2 and CO on Cu/SiO_2 support the contention that SO_2 chemisorbs on copper and prove that the present results could not have arisen because of SO_2 adsorbed on the alumina support influencing the behaviour of the copper component of the catalyst. Results for the alumina support presented here were only recorded as background data for the study of Cu/Al_2O_3 and are not believed to be relevant to the catalytic or adsorptive behaviour of the copper component of the catalysts.

CONCLUSIONS

(a) The ν_{CO} infrared band positions and adsorption and desorption behaviour of CO on Cu/Al_2O_3 catalysts shows that the relative strength of CO-adsorption sites are Cu^+ (in a Cu^{2+} matrix) > Cu^+ (in a Cu^+ matrix) > Cu^0. Some Cu^{2+} sites on calcined copper are reduced to Cu^+ either by evacuation at high temperature or by contact with CO at 295 K. Some Cu^+ sites on a $Cu^+O^{2-}Cu^+$ surface are reduced to Cu^0 by CO at 295 K.

(b) The adsorption of thiophene blocks CO adsorption on isolated Cu^{2+} sites but not on Cu^+ sites. However, thiophene on Cu^{2+} sites has an electronic strengthening effect on the adsorption of CO on vicinal Cu^+ sites. This relies on electron transfer from the π-electrons of the thiophene ring to Cu^{2+} surface cations.

(c) Thiophene on a $Cu^+O^{2-}Cu^+$ surface has predominantly an electronic rather than a site-blocking effect on CO adsorption.

(d) Thiophene adsorbs at low pressures on a Cu^0 surface in a parallel orientation to the surface which blocks CO adsorption. At higher pressures the thiophene rings adopt a perpendicular configuration which renders the copper surface sites more accessible to CO. Electron transfer from copper to the π-electron systems (parallel orientation) or the sulphur atoms (perpendicular orientation) of thiophene molecules generates surface atoms which behave in a way which is more typical of Cu^+ rather than Cu^0 towards CO adsorption.

(e) Surface complexes of thiophene with Cu^0 and Cu^+ surface sites are more stable than adsorbed thiophene-Cu^{2+} complexes.

(f) Sulphur dioxide poisons alumina and isolated Cu^{2+} sites in oxidised Cu/Al_2O_3 for the subsequent adsorption of CO.

(g) CO adsorbed on Cu^+ sites on a partially oxidised copper surface is influenced electronically by sulphur dioxide adsorbed on adjacent surface sites. Electron transfer from the copper surface to adsorbed species formed from SO_2 strengthens the C–O and weakens the Cu–C bonds in the adjacent carbonyl complex.

(h) SO_2 is dissociatively adsorbed on Cu^0 with resulting oxidation of copper sites and the generation of surface anions derived from SO_2. The SO_2 adsorption does not inhibit the adsorption of CO which interacts with the oxi-

dised copper sites in a way which is typical of CO adsorption on Cu/Al_2O_3 which had been partially oxidised by pretreatment with N_2O exposed to SO_2.

ACKNOWLEDGMENT

We thank SERC for a studentship and ICI Katalco for financial assistance.

REFERENCES

1. Hutchings, G. J., King, F., Okoye, I. P., and Rochester, C. H., *Appl. Catal.* **83,** L7 (1992).
2. Hutchings, G.J., King, F., Okoye, I. P., Padley, M. B., and Rochester, C. H., *J. Catal.* **148,** 453 (1994).
3. Hutchings, G. J., King, F., Okoye, I. P., Padley, M. B., and Rochester, C. H., *J. Catal.* **148,** 464 (1994).
4. Oudar, J., Pinol, S., Pradier, C. M., and Berthier, Y., *J. Catal.* **107,** 445 (1987).
5. Campbell, C. T., Koel, B. E., and Daube, K. A., *J. Vac. Sci. Technol., A* **5,** 810 (1987).
6. Fitzharris, W. D., Katzer, J. R., and Manogue, W. H., *J. Catal.* **76,** 369 (1982).
7. Ng, C. F., and Martin, G. A., *J. Catal.* **54,** 384 (1978).
8. Maclaren, J. M., Pendry, J. B., and Joyner, R. W., *Surf. Sci.* **178,** 856 (1986).
9. Maclaren, J. M., Vvedensky, D. D., Pendry, J. B., and Joyner, R. W., *J. Chem. Soc., Faraday Trans. 1* **83,** 1945 (1987).
10. Joyner, R. W., and Pendry, J. B., *Catal. Lett.* **1,** 1 (1988).
11. Maclaren, J. M., Vvedensky, D. D., Pendry, J. B., and Joyner, R. W., *J. Catal.* **110,** 243 (1988).
12. Lebedev, N. I., Mikhalenko, I. I., Kuzhel, L. M., and Yagodovkii, V. D., *Zh. Fiz. Khim.* **64,** 3365 (1990).
13. Somorjai, G. A., *J. Catal.* **27,** 452 (1972).
14. McCarroll, J. J., Edmonds, T., and Pitkethly, R. C., *Nature* **223,** 1260 (1969).
15. McCarroll, J. J., *Surf. Sci.* **53,** 297 (1975).
16. Bénard, J., *Catal. Rev.* **3,** 129 (1969).
17. Atrei, A., Johnson, A. L., and King, D. A., *Surf. Sci.* **254,** 65 (1991).
18. Bonzel, H. P., *Surf. Sci.* **27,** 387 (1971).
19. Richardson, N. V., and Campuzano, J. C., *Vacuum* **31,** 449 (1981).
20. Sexton, B. A., *Surf. Sci.* **163,** 99 (1985).
21. Saleh, J. M., *J. Chem. Soc., Faraday Trans. 1* **68,** 1520 (1972).
22. Baxter, J. P., Grunze, M., and Kong, C. W., *J. Vac. Sci. Technol., A.* **6,** 1123 (1988).
23. Leung, K. T., Zhang, X. S., and Shirley, D. A., *J. Phys. Chem.* **93,** 6164 (1989).
24. Apesteguia, C. R., Brema, C. E., Garetto, T. F., Borgna, A., and Parera, J. M., *J. Catal.* **89,** 52 (1984).
25. Argano, E. S., Randhava, S. S., and Rehmat, A., *Trans. Faraday Soc.* **65,** 552 (1969).
26. Rochester, C. H., and Terrell, R. J., *J. Chem. Soc., Faraday Trans. 1* **73,** 609 (1977).
27. Kohler, M. A., Cant, N. W., Wainwright, M. S., and Trimm, D. L., *J. Catal.* **117,** 188 (1989).
28. Fink, P., *Rev. Roum. Chim.* **14,** 811 (1969).
29. Parkyns, N. D., *J. Chem. Soc. A*, 410 (1969).
30. Parkyns, N. D., *J. Phys. Chem.* **75,** 526 (1971).
31. Amenomiya, Y., Morikawa, Y., and Pleizier, G., *J. Catal.* **46,** 431 (1977).
32. Rosynek, M. P., *J. Phys. Chem.* **79,** 1280 (1975).
33. Della Gatta, G., Fubini, B., Ghiotti, G., and Morterra, C., *J. Catal.* **43,** 90 (1976).
34. Morterra, C., Magnacca, G., Filippi, F., and Giachello, A., *J. Catal.* **137,** 346 (1992).
35. Parkyns, N. D., *J. Chem. Soc. A*, 1910 (1967).
36. Busca, G., and Lorenzelli, V., *Mater. Sci.* **7,** 89 (1982).
37. Morterra, C., Emanuel, C., Cerrato, G., and Magnacca, G., *J. Chem. Soc., Faraday Trans. 1* **88,** 339 (1992).
38. Griffiths, D. M., and Rochester, C. H., *J. Chem. Soc., Faraday Trans. 1* **74,** 403 (1978).
39. Griffiths, D. M., and Rochester, C. H., *J. Chem. Soc., Faraday Trans 1* **73,** 1913 (1977).
40. Pritchard, J., Catterick, T., and Gupta, R. K., *Surf. Sci.* **53,** 1 (1975).
41. Davydov, A. A., *Kinet. Katal.* **26,** 157 (1985).
42. Ulendeeva, A. D., Lygin, V. I., and Lyapina, N. K., *Kinet. Katal.* **20,** 978 (1979).
43. Padley, M. B., Rochester, C. H., Hutchings, G. J., and King, F., *J. Chem. Soc., Faraday Trans. 1* **90,** 203 (1994).
44. Madon, R. J., and Shaw, H., *Catal. Rev.—Sci. Eng.* **15,** 69 (1977).
45. Cloos, P., D. V., and Camerlynck, J. P., *Nature (London), Phys. Sci.* **243,** 54 (1973).
46. Sultanov, A. S., Khakimov, U. B., Talipov, G. S., and Shchenkochinin, J. M., *React. Kinet. Catal. Lett.* **2,** 243 (1975).
47. Datta, A., Cavell, R. G., Tower, R. W., and George, Z. M., *J. Phys. Chem.* **89,** 443 (1985).
48. Chang, C. C., *J. Catal.* **53,** 374 (1978).
49. Yao, H. C., Stepien, H. K., and Gandhi, H. S., *J. Catal.* **67,** 231 (1981).
50. Karge, H. G., and Dalla Lana, I. G., *J. Phys. Chem.* **88,** 1538 (1984).
51. Lokhov, Y. A., and Davydov, A. A., *Kinet. Katal.* **20,** 1498 (1979).
52. Fu, Y., Tain, Y., and Lin, P., *J. Catal.* **132,** 85 (1991).
53. Lokhov, Y. A., Sadykov, V. A., Tikhov, S. F., and Popovskii, V. V., *Kinet. Katal.* **26,** 177 (1985).
54. Tikhov, S. F., Paukshtis, E. A., Sadykov, V. A., Popovskii, V. V., Starostina, T. G., Kryukova, G. N., Kharlamov, G. V., Anufrienko, V. F., Poluboyarov, V. F., Razdobarov, V. A., Bulgakov, N. N., and Kalinkin, A. V., *Kinet. Catal. (Engl. Transl.)* **30,** 764 (1989).
55. Hierl, R., Urbach, H.-P., and Knözinger, H., *J. Chem. Soc., Faraday Trans. 1* **88,** 255 (1992).
56. Ghiotti, G., Boccuzzi, F., and Chiorino, A., *Stud. Surf. Sci. Catal.* **21,** 235 (1985).
57. Davydov, A. A., Prudnikova, O. Y., and Yur'eva, T. M., *Kinet. Katal.* **30,** 477 (1989).
58. Ertl, G., Hierl, R., Knözinger, H., Thiele, N., and Urbach, H. P., *Appl. Surf. Sci.* **5,** 49 (1980).
59. Martland, M. M., and Pinnavaia, T. J., *Nature (London), Phys. Sci.* **229,** 75 (1971).
60. Efremov, A. A., and Davydov, A. A., *Kinet. Katal.* **24,** 1180 (1983).
61. Newman, G., and Powell, D. B., *Spectrochim. Acta.* **19,** 213 (1963).
62. Kent, S. A., Katzer, J. R., and Manogue, W. H., *Ind. Eng. Chem. Fundam.* **16,** 443 (1977).
63. Millar, G. J., Rochester, C. H., and Waugh, K. C., *J. Chem. Soc., Faraday Trans. 1* **87,** 1467 (1991).
64. Efremov, A. A., Lokhov, Y. A., and Davydov, A. A., *Kinet. Katal.* **22,** 702 (1981).
65. Toolenaar, F. J. C. M., Stoop, F., and Ponec, V., *J. Catal.* **82,** 1 (1983).
66. Hierl, R., Knözinger, H., and Urbach, H.-P., *J. Catal.* **69,** 475 (1981).
67. Smith, A. W., and Quets, J. M., *J. Catal.* **4,** 163 (1965).
68. Kavtaradze, N. N., and Sokolova, N. P., *Russ. J. Phys. Chem. (Engl. Transl.)* **44,** 603 (1970).
69. Ghiotti, G., Boccuzzi, F., and Chiorino, A., *Surf. Sci.* **178,** 553 (1986).
70. Boccuzzi, F., Ghiotti, G., and Chiorino, A., *Surf. Sci.* **156,** 933 (1985).

71. Hollins, P., and Pritchard, J., *Surf. Sci.* **89,** 486 (1979).
72. Dumas, P., Tobin, R. G., and Richards, P. L., *J. Electron Spectrosc. Relat. Phenom.* **39,** 183 (1986).
73. Kohler, M. A., Cant, N. W., Wainwright, M. S., and Trimm, D. L., *J. Catal.* **117,** 188 (1989).
74. de Jong, K. P., Geus, J. W., and Joziasse, J., *Appl. Surf. Sci.* **6,** 273 (1980).
75. Roberts, D. L., and Griffin, G. L., *J. Catal.* **134,** 220 (1992).
76. Oudar, J., *Catal. Rev.—Sci. Eng.* **22,** 171 (1980).
77. Wong, J.-T., and Hoffmann, R., *J. Chem. Soc., Faraday Trans. 1* **86,** 553 (1990).
78. Sárkány, J., and Bartók, M., *Stud. Surf. Sci. Catal.* **48,** 845 (1989).
79. Sárkány, J., and Bartók, M., *Vacuum* **40,** 109 (1990).
80. Ford, R. R., *Adv. Catal.* **21,** 51 (1970).
81. Halachev, T., and Ruckenstein, E., *J. Catal.* **73,** 171 (1982).